Reconfigurable Microwave Photonic Filter with Linear Amplitude Response Based on Quantum Dash Optical Frequency Comb Source for Instantaneous Frequency Measurement

Yuxuan Xie [(1)], Mostafa Khalil [(1)], Jiaren Liu [(2),] Zhenguo Lu [(2)], Philip J. Poole [(2)], John Weber [(2)], and Lawrence R. Chen [(1)]

[(1)] McGill University, Montreal, Canada. yuxuan.xie@mail.mcgill.ca
[(2)] Advanced Electronics and Photonics Research Center, National Research Council Canada

Abstract *We experimentally demonstrate an instantaneous frequency measurement system based on a microwave photonic filter with linear amplitude responses (positive and negative slope). The overall rms error is 42.2 MHz in the range 2-20 GHz.*

Introduction

The instantaneous measurement of an unknown radio frequency (RF) signal is essential for wireless networks and electronic intelligence systems [1]–[4]. There are two typical methods for the measurement. First, the frequency-to-frequency mapping approach is specially designed for ultra-high frequency signals. By using the optical frequency comb (OFC) lines as a downconverter, a terahertz signal could be converted into a gigahertz level signal [3], which could be measured by a spectrum analyzer. On the other hand, frequency-to-amplitude mapping could simplify the frequency measurement into a power measurement problem. There are several devices to implement frequency-to-amplitude mapping. First, the frequency response of a photonic device, such as a Bragg grating [5], ring resonator [6], and Mach–Zehnder interferometer (MZI) [7], could map the frequency into the optical power. Furthermore, mapping the frequency into electrical power could be also a solution, in which a filter system, such as the microwave photonic (MWP) filter, is the most comment option [2]. However, the main limitation of the frequency-to-amplitude mapping method is one power may be mapped into more than one possible frequency [1], due to the periodic response of the devices. For the multi-band frequency measurement system, there are some blind spots between two nearby bands. One of the possible solutions is using more than one MWP filter response to do the measurement. By comparing the results between them, a unique measurement result could be obtained, and that method is called amplitude comparison function (ACF) [2]. Nevertheless, this operation will increase the complexity of the system. Ideal characteristics of the MWP filter response for frequency-to-power mapping include:

(1) a monotonic amplitude variation in the measurement range,
(2) a quick roll off to reduce error, and
(3) a linear variation.

In this paper, we experimentally demonstrate two MWP filters with linear amplitude frequency responses for frequency measurement. This MWP filter is implemented by a quantum dash (QDash) mode-locked laser (MLL) as the OFC source. With the help of a programable optical filter, the system is reconfigurable, and both positive and negative taps of the MWP filters are also achieved by using a balanced photodiode (BPD). These two MWP filters could work individually for frequency measurement with a root-mean-square error (RMSE) of about 55 MHz. Moreover, they can also work together as an ACF to reduce the measurement error to as low as 42.2 MHz.

System design

The principle of MWP filter is known as a finite impulse response (FIR) filter implemented with optical approaches. Thus, the overall MWP filter response *H(f)* can be described as followings [8]:

$$|H(f)| = \left|\cos\left(\frac{\pi {\lambda_0}^2 D}{c}\cdot f^2\right)\right| \cdot \left|\sum_{n=0}^{N-1} P_n \cdot exp\left(-jn2\pi \cdot \frac{f}{1/D\Delta\lambda}\right)\right| \quad (1)$$

where D is the fiber dispersion in ps/nm, λ_0 is the center operation wavelength, $\Delta\lambda$ is the comb wavelength spacing, and f is the RF frequency. P_n is a series that describes the power of all comb lines, e.g., P_0 is the power of the first comb line. The first term of Eq. 1 is the carrier suppression effect of the double sideband modulation (and can be avoided using single side band modulation), and the second is the filter response controlled by the comb shaping. Moreover, the second term is the discrete-time Fourier transform (DTFT) of the comb power series P_n. Therefore, this P_n can be determined using the MATLAB DSP toolbox [9], as it is the impulse response of any filter response we want. Note that the number of comb lines corresponds to the order of the FIR filter.

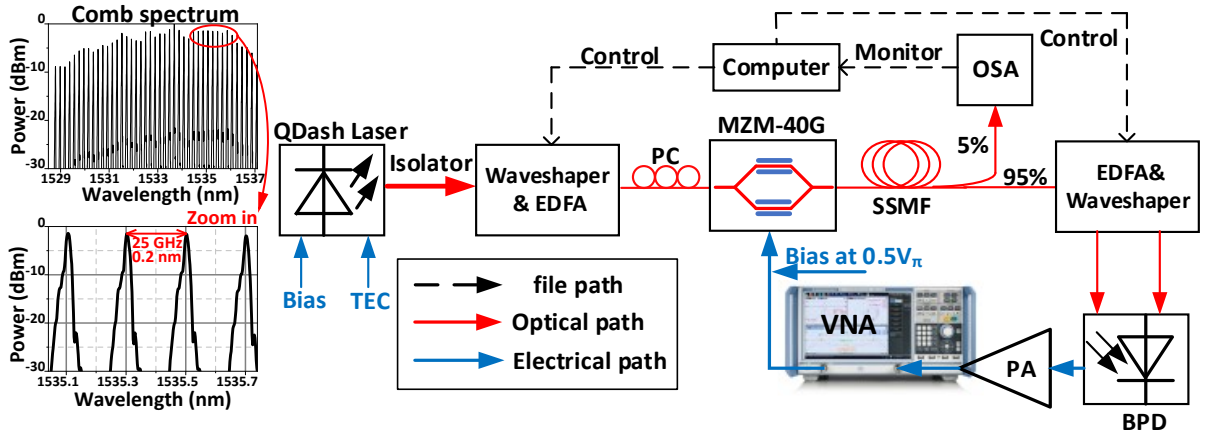

Fig. 1 Optical spectrum of QDash laser with an injection current of 292 mA in 22.5 ℃, and the system schematic. TEC: thermoelectric cooler, PC: polarization controller, EDFA: Erbium-doped fiber amplifier, MZM: Mach-Zehnder modulator, PA: (electrical) power amplifier

The OFC source used is an InAs/InP-based QDash MLL. The core area is a five-layer InAs quantum dash with a period of 108 Å surrounded by a p-type InP cladding. The schematic details are available in [10]. This QDash MLL has a threshold current of about 50 mA, and the pump current can be up to 400 mA. At the maximum bias current, the QDash MLL can generate more than 50 comb lines with a comb spacing of 25 GHz (0.2 nm) in the C-band [10]–[12]. Here, the QDash MLL is pumped at ~290 mA at room temperature (23 ℃). As illustrated in [13], there are 41 comb lines in the range 1529~1537 nm with 0.2 nm FSR.

Fig. 1 illustrates the experimental setup of our frequency measurement system. Overall, it is a typical intensity modulation and direct detection (IMDD) system with an OFC source. There are two waveshapers (Finisar waveshaper 1000s and 4000s) to complete the shaping for OFC lines and de-multiplexing. The first waveshaper performs power shaping of the OFC assisted by a control feedback loop, where the optical spectrum analyzer (OSA) is used as a monitor. To implement the negative taps of the MWP filter, the second waveshaper is used to de-multiplex all taps into two (positive and negative) channels which are then detected by a BPD [13]. It is important to note that a single waveshaper (4000s) can be used for both power shaping and de-multiplexing of the positive and negative taps. The delay medium of the MWP filter is a 3.2 km standard single mode fiber (SSMF), whose dispersion is about 17 ps/km·nm in the C-band. Next, the frequency response of the MWP filter is measured by a vector network analyzer (VNA) (R&S ZNB20) with a range of 0.5 MHz to 20 GHz and 1 MHz span. The measurement of the filter frequency response is repeated 100 times. Finally, after repeated measurements of the filter responses, we operate the VNA in constant wave (CW) mode to generate an unknown frequency and evaluate the error of the measurement system, using 2 GHz and 10 GHz as reference.

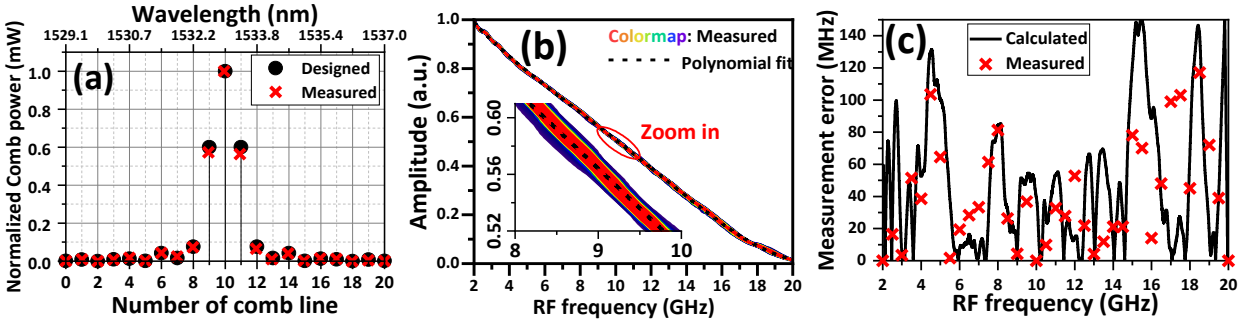

Fig. 2 (a) Spectrum of shaped comb lines with all positive taps. (b) frequency response of the MWP filter after subtracting the back-to-back (B2B) response after 100 times measurement. (c) calculated and measured errors.

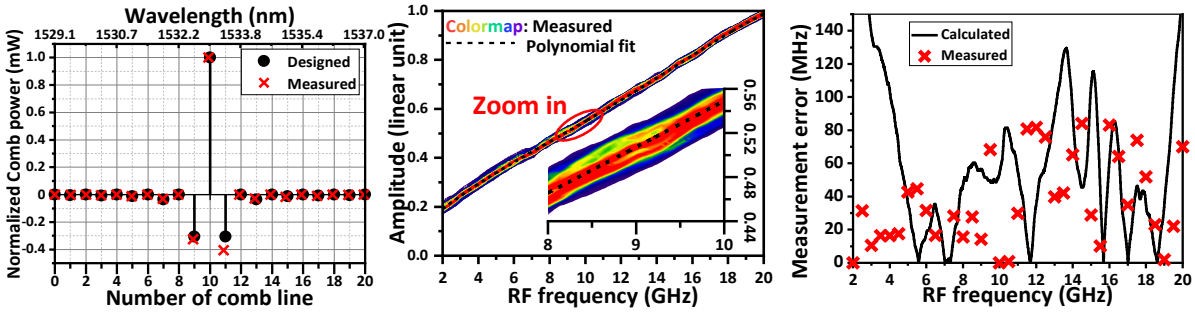

Fig. 3 (a) Spectrum of shaped comb lines with positive and negative taps. (b) frequency response of the MWP filter after subtracting the back-to-back (B2B) response after 100 times measurement. (c) calculated and measured errors.

Results and discussion

First, to let the system operate up to 20 GHz, the comb spacing must be 50 GHz since the maximum operating frequency is half of the comb spacing. Thus, we use the waveshaper to select one comb line from every two comb lines to obtain a group of 21 new comb lines with 50 GHz spacing. When all positive taps are used, the shaping of the comb lines is a sinc squared function—see Fig. 2 (a)—to obtain an MWP with a linear amplitude response in linear units (e.g., mW). The corresponding filter response, after accounting for the back-to-back (B2B) system response (modulator and fiber), is shown in Fig. 2 (b), i.e., the response corresponding to the second term in Eq. 1. The measurement is repeated 100 times, shown by the colormap in Fig. 2 (b). Furthermore, the RMSE of these 100 samples is calculated and presented in the solid line of Fig. 2 (c). However, this result should be treated as the worst case of our system. In practice, we would measure the average power obtained from multiple measurements. Here, we start from 2 GHz to 20 GHz in steps of 0.5 GHz to mimic an unknown frequency measurement, and the results are shown as the red crosses in Fig. 2 (c), where the overall RMSE is just 51.1 MHz.

For all positive taps, the slope of the filter response is negative, which indicates that a higher frequency is mapped into a lower power. To improve the accuracy in the high-frequency range, a filter response with a positive slope is required. To achieve such a filter, a comb shaping with both positive and negative taps is required, as shown in Fig. 3 (a). After measuring 100 times and accounting for the B2B response, a linear filter with a positive slope is obtained in Fig. 3 (b). The RMSE of the measurement is 58.1 MHz, see Fig. 3 (c).

As a reconfigurable system, these two linear filters could even work together to improve accuracy. With the ACF method, no reference signal is required. By using two filters to do the measurement and take an average, the overall RMSE is reduced to 42.2 MHz, as plotted in Fig. 4. This RMSE is comparable to that obtained in [2], though we only require two MWP filter responses to implement the ACF.

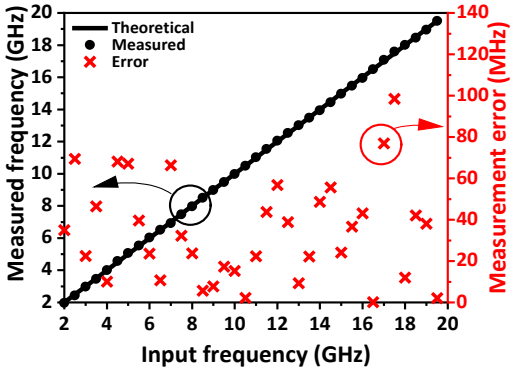

Fig. 4 Measured frequencies (black dots) by using two filters together, and the measurement error (red crosses).

Conclusions

In this paper, we have proposed and experimentally demonstrated a frequency measurement system based on frequency-to-power mapping with MWP filters having linear amplitude responses. The system is reconfigurable, and it allows two linear filter responses to be obtained and when working together to implement an ACF, a frequency measurement with RMSE 42.2 MHz is obtained.

Acknowledgments

We thank the High Throughput and Secure Networks Challenge Program at the National Research Council of Canada, CMC Microsystems, and the Institut National de la Recherche Scientifique (INRS) for their support.

References

[1] M. Pagani, B. Morrison, Y. Zhang, A. Casas-Bedoya, T. Aalto, M. Harjanne, M. Kapulainen, B. J. Eggleton, and D. Marpaung, “Low-Error and Broadband Microwave Frequency Measurement in a Silicon Chip,” *Optica*, vol. 2, no. 8, p. 751, Aug. 2015, doi: 10.1364/OPTICA.2.000751.

[2] E. Nazemosadat, S. García, and I. Gasulla, “Heterogeneous Multicore Fiber-Based Microwave Frequency Measurement,” *Optics Express*, vol. 30, no. 15, p. 26886, Jul. 2022, doi: 10.1364/OE.463152.

[3] I. Morohashi, I. Katayama, M. Kirigaya, Y. Irimajiri, N. Sekine, and I. Hosako, “High Precision Frequency Measurement of Terahertz Waves Using Optical Combs from a Mach–Zehnder-Modulator-Based Flat Comb Generator,” *Optics Letters*, vol. 44, no. 3, p. 487, Feb. 2019, doi: 10.1364/OL.44.000487.

[4] X. Zou, S. Pan, and J. Yao, “Instantaneous Microwave Frequency Measurement with Improved Measurement Range and Resolution Based on Simultaneous Phase Modulation and Intensity Modulation,” *Journal of Lightwave Technology*, vol. 27, no. 23, pp. 5314–5320, Dec. 2009, doi: 10.1109/JLT.2009.2030695.

[5] Z. Li, C. Wang, M. Li, H. Chi, X. Zhang, and J. Yao, “Instantaneous Microwave Frequency Measurement Using a Special Fiber Bragg Grating,” *IEEE Microwave and Wireless Components Letters*, vol. 21, no. 1, pp. 52–54, Jan. 2011, doi: 10.1109/LMWC.2010.2091114.

[6] L. Liu, W. Xue, and J. Yue, “Photonic Approach for Microwave Frequency Measurement Using a Silicon Microring Resonator,” *IEEE Photonics Technology Letters*, vol. 31, no. 2, pp. 153–156, Jan. 2019, doi: 10.1109/LPT.2018.2886894.

[7] J. S. Fandiño and P. Muñoz, “Photonics-Based Microwave Frequency Measurement Using a Double-Sideband Suppressed-Carrier Modulation and an Inp Integrated Ring-Assisted Mach–Zehnder Interferometer Filter,” *Optics Letters*, vol. 38, no. 21, p. 4316, Nov. 2013, doi: 10.1364/OL.38.004316.

[8] L. R. Chen and V. Pagé, “Tunable Photonic Microwave Filter Using Semiconductor Fibre Laser,” *Electronics Letters*, vol. 41, no. 21, p. 1183, 2005, doi: 10.1049/el:20052952.

[9] MATLAB, “Design Filters Starting with Algorithm Selection - Matlab.” Accessed: Feb. 05, 2023. [Online]. Available: https://www.mathworks.com/help/signal/ref/filterdesigner-app.html

[10] Z. Lu, J. Liu, P. J. Poole, Y. Mao, J. Weber, G. Liu, and P. Barrios, “InAs/InP Quantum Dash Semiconductor Coherent Comb Lasers and Their Applications in Optical Networks,” *Journal of Lightwave Technology*, vol. 39, no. 12, pp. 3751–3760, Jun. 2021, doi: 10.1109/JLT.2020.3043284.

[11] K. Zeb, Z. Lu, J. Liu, Y. Mao, G. Liu, P. J. Poole, M. Rahim, G. Pakulski, P. Barrios, W. Jiang, and X. Zhang, “InAs/InP Quantum Dash Buried Heterostructure Mode-Locked Laser for High Capacity Fiber-Wireless Integrated 5g New Radio Fronthaul Systems,” *Optics Express*, vol. 29, no. 11, p. 16164, May 2021, doi: 10.1364/OE.424504.

[12] P. J. Poole, K. Kaminska, P. Barrios, Z. Lu, and J. Liu, “Growth of InAs/InP-Based Quantum Dots for 1.55μm Laser Applications,” *Journal of Crystal Growth*, vol. 311, no. 6, pp. 1482–1486, Mar. 2009, doi: 10.1016/j.jcrysgro.2009.01.129.

[13] H. Sun, M. Khalil, J. Liu, Z. Lu, P. J. Poole, J. Weber, D. V. Plant, and L. R. Chen, “Reconfigurable Microwave Photonic Filter Based on a Quantum Dash Mode-Locked Laser,” *Optics Letters*, vol. 47, no. 5, p. 1133, Mar. 2022, doi: 10.1364/OL.451185.